GeoAmericas2020
4th PAN AMERICAN CONFERENCE ON GEOSYNTHETICS
26-29 APRIL 2020 • RIO DE JANEIRO • BRAZIL

# A new design method for working platforms stabilised by multi-axial geogrid

A.S. Lees, Tensar International, Nicosia, Cyprus
M. Wayne, Tensar Corporation, Alpharetta, GA
G. Fountain, Tensar Corporation, San Diego, CA.

ABSTRACT
The design of working platforms typically involves the calculation of a two-layer bearing capacity. Existing calculation models are quite empirical with imprecise input parameters while other proposed methods have tended to involve multiple design charts and been suited to either strip or circular foundations only. It has also been difficult to incorporate the benefits of geosynthetics in an accurate way. The recently developed "T-Value Method" defines bearing capacity simply in terms of the ratio of strengths of the two layers. It also allows realistic incorporation of the benefit of multi-axial stabilising geogrid in terms of the enhanced shear strength of the upper granular layer. This is leading to significant cost savings due to thinner working platforms that are designed in a safe and scientifically rigorous way. The greater ductility of stabilised granular layers also provides greater assurance that the assumed failure mechanisms can be fully mobilised before strain softening in the granular layer occurs. This paper summarises the development of this new design method and describes some of the full-scale field tests that have been used in its validation.

## 1. NOTATION

| | |
|---|---|
| $B$ | Foundation width or diameter |
| $D$ | Foundation embedment depth |
| $H$ | Granular layer thickness between foundation base and clay |
| $L$ | Foundation length |
| $T$ | Granular layer load transfer efficiency |
| $p'_0$ | Effective vertical stress at base of granular layer |
| $q_g$ | Net bearing capacity of granular layer of infinite depth |
| $q_s$ | Surface bearing capacity of clay |
| $q_u$ | Net bearing capacity of granular layer on clay |
| $s_u$ | Undrained shear strength of clay |
| $\alpha$ | Load spread angle |
| $\gamma$ | Weight density of granular layer |
| $\varphi'$ | Internal friction angle of granular layer |

## 2. INTRODUCTION

Working platforms are currently constructed with mechanically stabilized soil for applications which include but are not limited to:

- Access & operations of heavy construction vehicles
- Temporary operation of cranes and foundation stabilization equipment
- Bridging of localized soft areas for construction access
- Capping of soft deposits
- Reduced excavation of unsuitable material
- Minimized export removal of unsuitable or contaminated material
- Accelerated construction time

The use of mechanical stabilisation has been proven to promote a safe and cost-effective solution for many industries by allowing contractors to quickly access, stabilise and utilize areas with unsuitable ground conditions all while saving the owner money in the process. A case in point is the use of a working platform for construction of a crane bearing pad for a petrochemical plant in Lake Charles, Louisiana (Tensar, 2017). The pad was installed on time despite heavy seasonal rains. Unlike their planned use of a concrete platform, the use of geogrid stabilised aggregate made it possible for removal and reuse at other locations on the site. The crane utilising the mechanically stabilised platform was rated as the 3rd largest in the world and withstood Hurricane Harvey without damage. The drainage system built into the construction platform allowed the crane to operate the day after the storm passed and the solution resulted in a cost savings of more than 3 million US dollars. Although the design of these platforms has evolved over the years, they follow a similar path.

The first step involves examination of what would lead to the bearing capacity failure of working platform. This occurs due to punching shear through the granular layer and a bearing capacity mechanism in the underlying clay (as illustrated in Figure 1), unless the granular layer exceeds a critical thickness above which shear failure occurs entirely within the upper layer. Existing design methods (without geogrid) include the semi-empirical Meyerhof (1974) or Hannah and Meyerhof (1980) method which are considered generally accurate for surface loads with low base to length, or *B*/*L* ratios, but suffers from the drawback that punching shear coefficients were derived empirically from model footing tests at 1g and not in a non-dimensional form. As such, they are appropriate only for the granular layer density and thickness used in the derivation (Burd & Frydman, 1997).

Alternatively, a simple load spread or projected area method is used where the granular layer is assumed to spread load uniformly to the underlying clay and the shear strength contribution of the granular layer is ignored (Terzaghi and Peck 1948; Yamaguchi 1963). The angle $\alpha$ of load spread to the vertical is assumed the same as the angle of the straight shear planes in the granular layer. Many values have been proposed, as summarised by Craig and Chua (1990), and the main drawback of this method is the difficulty of determining $\alpha$. Brocklehurst (1993) and Ballard et al (2011) showed that α is also influenced by the shear strength of both the granular layer and the underlying clay.

Lees (2019) derived a non-dimensional relationship (Equations 1 and 2) between bearing capacity ratio $q_u/q_s$ and the load transfer efficiency of the granular layer expressed as a dimensionless T value. The T value depends on the shear strengths of the two layers and these relationships are derived by numerical analysis (e.g. finite element analysis (FEA)) parametric study and physical testing, the results of which are shown as the lower non-stabilised curves in Figure 2. In design, this allows a simple calculation to be made of the bearing capacity directly from the shear strengths of the individual soil layers without the need for empirical-based charts. It can be applied to both surface and shallow embedded foundations, circular and rectangular and with dry or saturated granular layers. The bearing capacity of foundations with *B*/*L* ratios between 0 and 1 can be determined by linear interpolation. The inequalities in Equations 1 and 2 are needed to check for cases where shear failure entirely within the granular layer is critical.

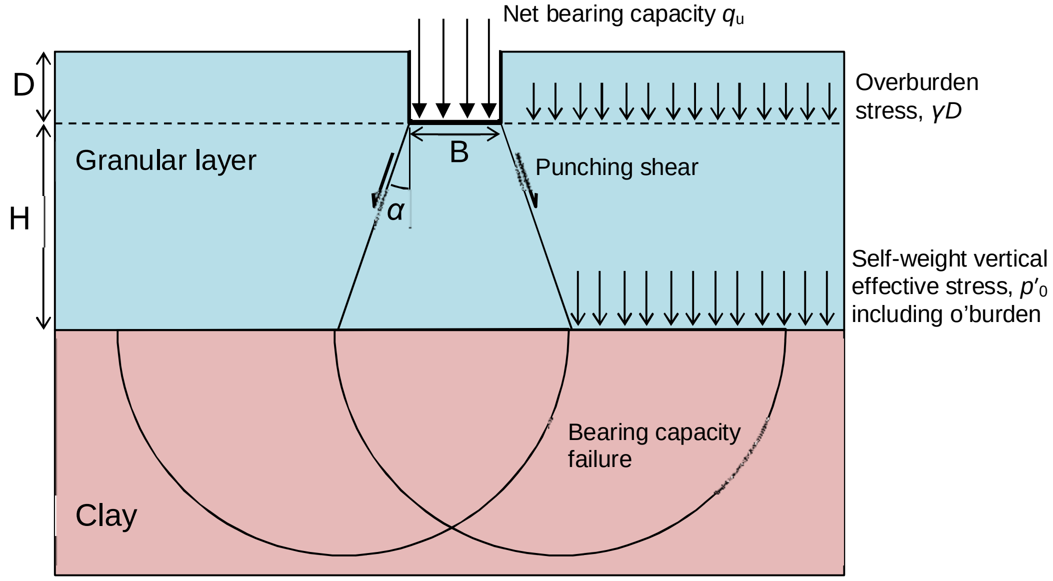


Figure 1. Geometry and terminology of working platform design.

$$\frac{q_u}{q_s} = 1 + T\frac{H}{B} \leq \frac{q_g}{q_s} \quad \text{(strip footing)} \qquad [1]$$

$$\frac{q_u}{q_s} = \left(1 + T\frac{H}{B}\right)^2 \leq \frac{q_g}{q_s} \quad \text{(square or circular footing)} \qquad [2]$$

The Meyerhof (1974) and load spread methods have both been modified to include the benefit of installing geogrid within the granular layer. A simple modification to the former was proposed in BRE (2004) involving the addition of a factored geogrid tensile strength to the design equation while Milligan et al (1989a and b) added the geogrid benefit to the load spread method by taking account of additional shear stresses generated at the interface between the granular layer and clay, limited by the tensile strength of the geogrid. These methods are intended for reinforcing geogrid where geogrid performance is defined in terms of a tensile strength obtained by testing in air. They are not suited to multi-axial geogrid that is designed primarily to stabilise the aggregate rather than provide tensile reinforcement. As reported by FHWA (2001), Westergaard's elastic layer theory, based on the assumption that the soil is stabilised by closely spaced stiff horizontal layers which prevent horizontal displacement of the surrounding soil, can be utilized to determine the stresses exerted below a closely spaced geogrid stabilised layer. The steps for utilizing this approach are also highlighted by the FHWA and as such will not be discussed further in this paper.

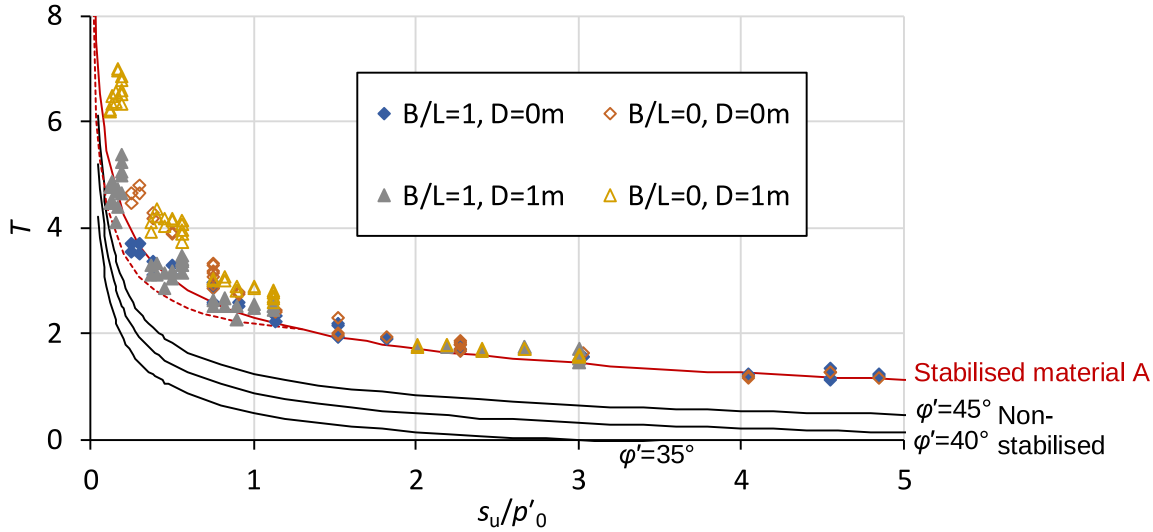


Figure 2. Variation of $T$ with $s_u$ for specific geogrid product and aggregate.

This paper addresses this drawback by presenting a modification to the new "T-Value Method" (Lees, 2019) to include the benefit of installing multi-axial stabilising geogrid in a granular layer overlying clay on its bearing capacity. The dependency of the stabilisation benefit on geometrical parameters and $s_u$ will be determined by finite element analysis (FEA) validated by full-scale testing.

## 3. STABILISED SOIL BEHAVIOUR

Stiff, punched and drawn multi-axial polypropylene (PP) geogrid was designed primarily to restrict the movement of soil particles in and around its apertures – a function defined as stabilisation in the International Geosynthetic Society's latest guide (IGS, 2018) – and there is evidence (e.g. Bussert and Cavanaugh (2010)) that the stabilising effect of geogrid extends a significant distance from the geogrid plane, typically 30 cm or more.

Lees and Clausen (2019) performed large triaxial compression tests (specimen size 0.5 m dia. x 1.0 m height) with vacuum-applied confining stress on a dry, crushed diabase rock with and without a stiff, punched and drawn multi-axial PP geogrid placed at mid-height. The crushed rock had a coefficient of uniformity $C_U$ of 23 with $D_{60}$ = 8 mm and $D_{100}$ = 40mm. It was compacted to at least 95% maximum dry density. The plots of averaged deviatoric stress $q$ against averaged axial strain

$\varepsilon_a$ at three different confining stresses with and without the geogrid in Figure 3 show an enhanced peak shear strength in the geogrid-stabilised soil at all three confining stresses. These formed a markedly non-linear failure envelope in the stabilised case due to restraint on particle translation and rotation, significantly increasing the work required to shear and dilate the specimen. Also of note is the larger strains required to cause significant softening of the stabilised granular soil compared with the non-stabilised case. Peak failure occurred at axial strains of about 4 to 5% in the non-stabilised case after which dilation-induced softening occurred whereas the stabilised specimens experienced significant softening at more than about 10% axial strain. Strain levels at the onset of bearing capacity failure in clays are generally up to about 10% depending on the clay stiffness, meaning that lower post-peak shear strengths are appropriate for overlying non-stabilised granular layers when calculating bearing capacity for design but, in many more cases, it would be appropriate to adopt the peak strength of stabilised granular layers due to the higher strain level at which significant strength softening occurs.

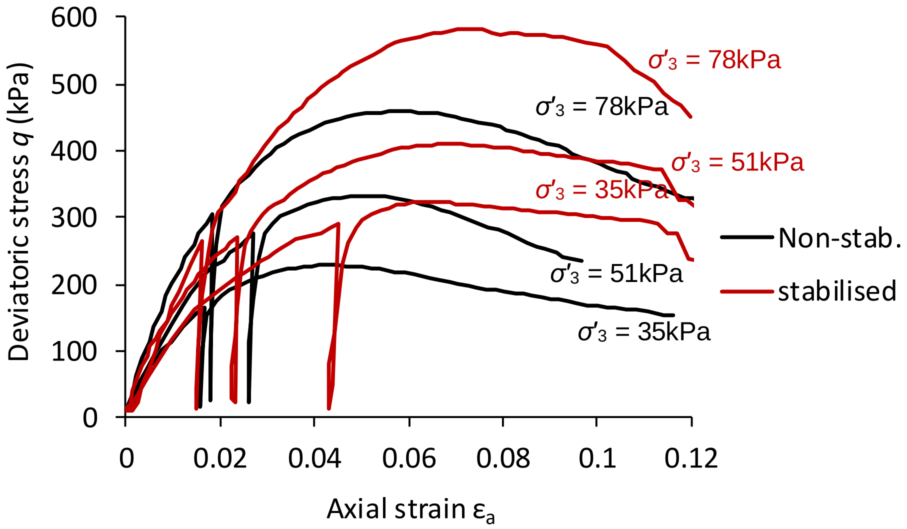


Figure 3. $q$ v. $\varepsilon_a$ plots from triaxial compression tests on stabilised and non-stabilised crushed rock aggregate.

Since the restraint on soil particles would be at a maximum at the geogrid plane and reduce with distance from the plane, the failure envelope was considered to vary (assumed linearly) from a maximum at the geogrid plane to the non-stabilised failure envelope at a perpendicular distance $\Delta y$, beyond which the non-stabilised failure envelope prevailed, as illustrated in Figure 4. The non-stabilised failure envelope can be obtained straightforwardly from shear strength tests on the granular material without geogrid and the maximum failure envelope and $\Delta y$ determined from the back analysis of shear strength tests with one or more layers of the specific geogrid product being tested.

A linear elastic perfectly-plastic (LEPP) constitutive model called the Tensar Stabilised Soil Model (TSSM) with the non-linear failure envelope was implemented into the Plaxis 2D 2018 (Brinkgreve et al, 2018) FEA software and found to provide accurate predictions of failure stress in back-analyses of the triaxial compression tests (Lees and Clausen, 2019).

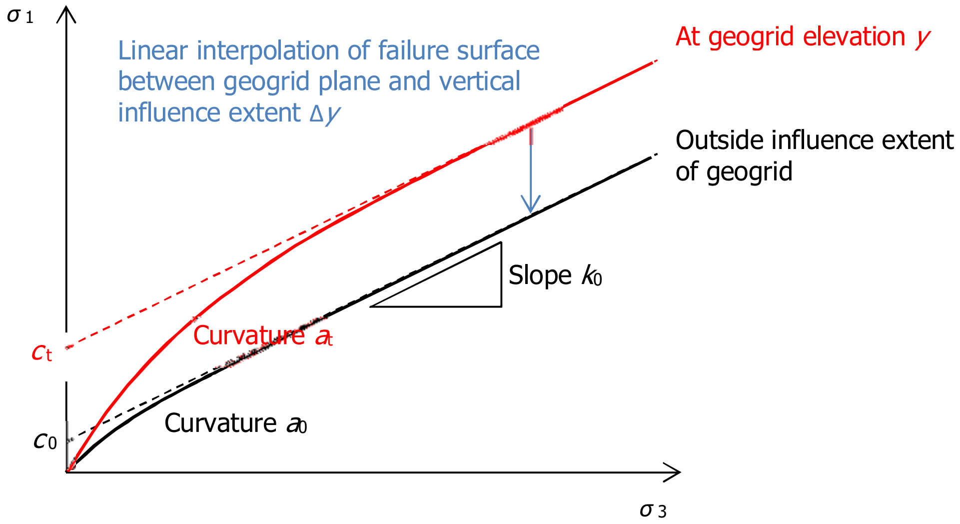


Figure 4. Geogrid-stabilised soil failure envelope (Lees and Clausen, 2019).

## 4. FEA PARAMETRIC STUDY

The parametric study of bearing capacity was performed by two-dimensional FEA using Plaxis 2D 2018 in plane strain for strip loads and axisymmetry for equivalent square loads. The TSSM was used for the granular material described in the previous section with a specific stabilising punched and drawn PP multi-axial geogrid denoted together as “Stabilised Material A” with the input parameters shown in Table 1. The clay was modelled with an LEPP model with Tresca failure criterion with undrained Young’s modulus $E_u$ taken as $800s_u$ and Poisson’s ratio $\nu_u$ as 0.495. Geometrical and clay shear strength parameters were varied as shown in Table 2 (the square footing $B$ values give the same foundation area as the circular footing simulated in FEA). In all cases, one geogrid plane was placed at the base of the granular layer. When $H$ was 0.45 and 0.6 m, an additional geogrid plane was placed 0.3 m above the base of the granular layer, and when $H$ was 0.75 and 0.9 m, a third geogrid plane was placed at 0.6 m above the base of the granular layer. A rigid, rough footing was assumed in all cases and displacement control was used to increase the load to failure.

Table 1. TSSM input parameters for Stabilised Material A.

| Parameter | Value |
|---|---|
| $k$ | 5.7 |
| $c_0$ | 56 kPa |
| $a_0$ | 2.0 |
| $M$ | 5.7 |
| $B$ | 2.0 |
| $\Delta y$ | 0.30 m |
| $c_t$ | 350 kPa |
| $a_t$ | 14 |
| $E$ | 50 MPa |
| $\nu$ | 0.25 |
| $\gamma$ | 21 kN/m$^3$ |

Table 2. Input parameters varied in the FEA parametric study.

| | |
|---|---|
| $s_u$ (kPa) | 5, 15, 30, 80 |
| $B/L$ | 0 (plane strain), 1 (axisymmetric) |
| $B$ (m) | 0.3, 0.6, 0.9, 1.2, 1.8, 2.4 |
| $H$ (m) | 0.3, 0.45, 0.6, 0.75, 0.9 |
| $\gamma D$ (kPa) | 0, 20 |

The output from the parametric study is presented in Figure 2 in terms of the $T$ value back-calculated using Equations 1 and 2 from output of $q_u$ and adopting $N_c$ = 5.14 and 6.2 for $q_s$ in the plane strain and axisymmetric cases respectively. All cases, including with overburden stress ($\gamma D$>0), are shown to follow a similar trend when $s_u$ is normalised by $p'_0$. The line shown is considered a best fit line for the plane strain ($B/L$=0) cases and a lower bound for the axisymmetric cases ($B/L$=1) and follows Equation 3 and can be applied for granular materials of similar characteristics with the specific geogrid product tested. The interactions between aggregates and geogrid are highly complex so similar products may not follow this relationship and should be derived specifically for each product following the same procedure with full-scale validation.

$$T = 2.9\left(\frac{s_u}{p'_0}\right)^{-0.32} - 0.6 \qquad [3]$$

The line follows a similar trend to those derived for non-stabilised granular layers with different $\varphi'$ angles shown where the $T$ value increases with the $\varphi'$ value. The higher $T$ value obtained with a stabilised granular layer is consistent with the higher shear strength imparted to the soil by the stabilising geogrid. The higher ductility of the stabilised granular layer also allows the peak strength to be used in design whereas for non-stabilised soil the strain levels at bearing capacity failure typically exceed peak failure strains in dense granular materials and post-peak shear strengths should be used in design.

The outputs of $T$ value become increasingly sensitive to $s_u/p'_0$ as $s_u/p'_0$ values fall below about 1.25 since stress changes have a proportionally bigger effect on bearing capacity as shear strength becomes very low. At $s_u/p'_0$ values below 1.25, it is recommended to apply the correction shown in Equation 4 to the $T$ value to take account of this uncertainty. This correction plots as the dashed line in Figure 2 which forms a lower bound to all the values obtained in the FEA parametric study. Alternatively, more advanced analysis (e.g. FEA) than the T-value method could be undertaken for bearing capacity calculations in very soft clays.

$$T_{corr} = \frac{T}{1+0.2(1.25-s_u/p'_0)} \quad \text{when } s_u/p'_0 < 1.25 \qquad [4]$$

## 5. VALIDATION

The stabilisation function of geogrid and enhanced shear strength are heavily dependent on the interactions between geogrid components and the aggregate particles that are being restrained. As such, the T-value to subgrade strength relationship should be derived for specific geogrid products and aggregate types and then validated by full-scale testing appropriate for the foundation or track width to be supported. An example of an appropriate full-scale validation test is presented in this section.

A 0.4 m thick platform of the same characteristics as "Stabilised Material A" including one layer of the multi-axial stabilising geogrid at its base was laid and compacted over the existing ground during construction of the Kingsway Business Park in Rochdale, UK in December 2018. The existing ground was a reworked Made Ground comprised of a firm gravelly clay to about 4 m depth.

Five plate load tests (PLT) on the platform surface were undertaken in accordance with BS 1377-4 Clause 4.1 (BSI, 1990). A large 600 mm diameter plate was used for the tests to match the expected loaded width on the platform and to ensure that the critical failure mechanism was punching shear through to the subgrade rather than shear failure entirely within the granular layer. Dynamic cone penetrometer (DCP) testing was also undertaken in accordance with Jones (2004) at each PLT location to confirm the platform thickness and to determine the $s_u$ value of the subgrade. Since $s_u$ is related to moisture content and varies, it is important to take measurements on the same day as the PLTs and the simple, lightweight nature of the DCP allows this on a live construction site. However, correlations between blow count and $s_u$ are approximate, especially for soft, fine-grained materials and results are subject to rod alignment and skin friction as well as operator error.

The results of the DCP testing are presented in Figure 5 as blows per 100 mm penetration where the 0.4 m thick platform is apparent. An average value for the subgrade is shown for which an $s_u$ value of 20 kPa was derived using Look (2014).

The bearing capacity of a 600 mm diameter plate on a 0.4 m thick platform of Stabilised Material A on a subgrade of $s_u$ = 20 kPa was calculated as 585 kPa using the method presented in this paper. The PLT results are plotted in Figure 6 where it is shown that the bearing pressure reached the approximate calculated bearing capacity on all 5 occasions without any indication of bearing failure visible on site or apparent in the load-deflection data. The load could not be increased further in an attempt to measure the fully mobilised bearing capacity because the safe capacity of the test equipment had been reached. Nevertheless, the actual bearing capacity exceeded the calculated value which provided useful validation of the proposed design method.

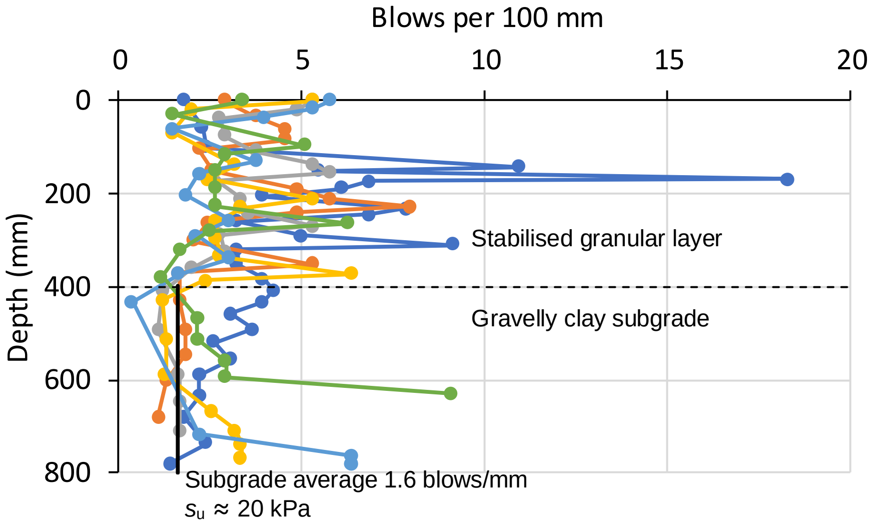


Figure 5. Dynamic cone penetrometer data from Rochdale, UK site.

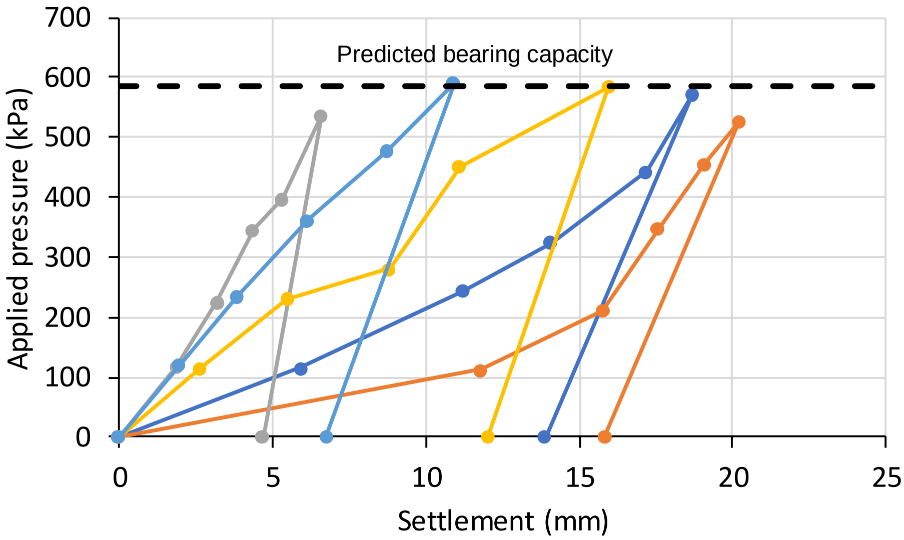


Figure 6. Plate load test data from Rochdale, UK site

## 6. CONCLUSIONS

A parametric study using FEA of strip and circular foundations was used to derive the load transfer efficiency *T* of a granular layer stabilised by a multi-axial PP geogrid product overlying a clay soil of a range of $s_u$ values. This relationship between *T* and $s_u$ can be used to calculate the bearing capacity of granular layers of similar characteristics stabilised with the specific geogrid product for a wide range of geometries and clay strengths. This has been demonstrated by a worked example and validated by comparison with an example full-scale field test.

The relationship between *T* and $s_u$ can be determined for other granular materials and stabilising geogrid products by 2D axisymmetric and plane strain FEA parametric studies covering the range of $s_u$ and *H*/*B* values that will be encountered, validated by full-scale testing with the same geogrid product and aggregate characteristics. FEA input parameters should be derived from large triaxial compression tests on the granular material at the appropriate density with the specific geogrid product.

This method provides engineers a quantifiable design method for determining increased bearing capacity for a 2-layer system constructed with mechanical stabilisation.

## REFERENCES

Ballard J-C, Delvosal P, Yonatan P, Holeyman A & Kay S, 2011. Simplified VH equations for foundation punch-through sand into clay. *Frontiers in Offshore Geotechnics II (ed. Gourvenec & White)*. CRC, London: 655-660.

BRE, 2004. BR470 *Working platforms for tracked plant*. BRE: Watford.

BRE, 2011. *Use of 'structural geosynthetic reinforcement' – A BRE review seven years on.* BRE: Watford.

Brinkgreve RBJ, Kumarswamy S, Swolfs WM & Foria F, 2018. *Plaxis 2018*. Delft.

Brocklehurst CJ, 1993. Finite element studies of reinforced and unreinforced two-layer soil systems, D.Phil thesis, University of Oxford.

BSI (1990) Methods for test for soils for civil engineering purposes. In-situ tests. BS 1377-9:1990. British Standards Institution, London.

Burd HJ & Frydman S, 1997. Bearing capacity of plane-strain footings on layered soils, *Canadian Geotechnical Journal* **34(2)**: 241-253.

Bussert F & Cavanaugh J, 2010. Recent research and future implications of the actual behaviour of geogrids in reinforced soil. ASCE Earth Retention Conference (ER2010), 1-4 August, Bellevue, Washington, p. 460-477.

Craig WH & Chua K, 1990. Deep penetration of spud-can foundations on sand and clay. *Géotechnique* **40(4)**: 541-556.

FHWA (2001) FHWA-NHI-01-023 *Shallow Foundations Reference Manual,* National Highway Institute, Washington, D.C.

Hannah AM & Meyerhof GG, 1980. Design charts for ultimate bearing capacity of foundations on sand overlying soft clay. *Canadian Geotechnical Journal* **17(2)**: 300-303.

IGS. (2018). Guide to the Specification of Geosynthetics, 5th edition. International Geosynthetics Society, Jupiter FL.

Jones C (2004) Dynamic cone penetrometer test and analysis. Project Report PR/INT/277/04. Transport Research Laboratory, Crowthorne, Berkshire.

Lees AS (2019) The bearing capacity of a granular layer on clay. *Proceedings of the Institution of Civil Engineers – Geotechnical Engineering* https://doi.org/10.1680/jgeen.18.00116 In press.

Lees AS & Clausen J, 2019. The strength envelope of granular soil stabilised by multi-axial geogrid in large triaxial tests. *Canadian Geotechnical Journal* https://doi.org/10.1139/cgj-2019-0036 In press.

Look BG (2014) *Handbook of Geotechnical Investigation and Design Tables*, 2nd edition. Taylor & Francis Group, Boca Raton, FL.

Meyerhof GG, 1974. Ultimate bearing capacity of footings on sand layer overlying clay. *Canadian Geotechnical Journal* **11(2)**: 223-229.

Milligan GWE, Jewell RA, Houlsby GT & Burd HJ, 1989a. A new approach to the design of unpaved roads – Part I. *Ground Engineering* **22** (April): 25-29.

Milligan GWE, Jewell RA, Houlsby GT & Burd HJ, 1989b. A new approach to the design of unpaved roads – Part II. *Ground Engineering* **22** (November): 37-42.

Tensar (2017) Case Study Petrochemical crane project, Lake Charles, LA

Terzaghi K & Peck RB, 1948. *Soil Mechanics in Engineering Practice*, 1st ed. John Wiley and Sons, New York.

Yamaguchi H, 1963. Practical formula of bearing value for two layered ground. In *Proceedings of the 2nd Asian Regional Conference of Soil Mechanics and Foundation Engineering, Tokyo*: 99–105.